

OPEN ACCESS

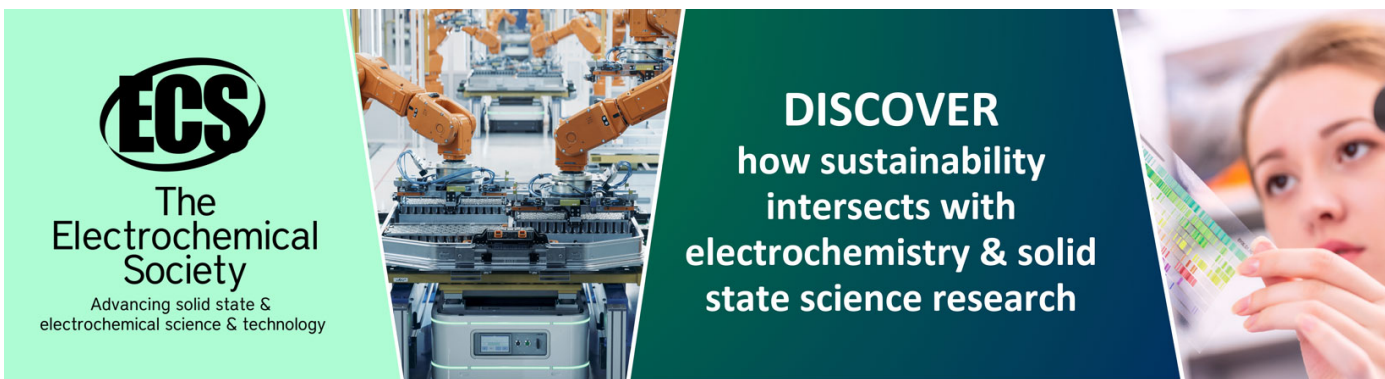
Annealing induced changes in ternary nanostructured $Zn_xCd_{1-x}Se$ thin films: structure and morphology

To cite this article: I Bineva *et al* 2012 *J. Phys.: Conf. Ser.* **398** 012015

View the [article online](#) for updates and enhancements.

You may also like

- [Effect of zinc concentration on the structural, electronic and elastic properties of \$Zn_xCd_{1-x}O\$ dilute alloys](#)
Brahim Bahloul and Lynda Amirouche
- [Investigation of \$Zn_xCd_{1-x}O\$ films bandgap and \$Zn_xCd_{1-x}O/ZnO\$ heterojunctions band offset by x-ray photoelectron spectroscopy](#)
Jie Chen, , Xue-Min Wang et al.
- [Reverse bandgap-bowing in nickel-cadmium sulfide alloys \(\$Ni_xCd_xS\$ \) and its origin](#)
Subham Paramanik, Soumyo Chatterjee and Amlan J Pal



ECS
The Electrochemical Society
Advancing solid state & electrochemical science & technology

DISCOVER
how sustainability intersects with electrochemistry & solid state science research

Annealing induced changes in ternary nanostructured $Zn_xCd_{1-x}Se$ thin films: structure and morphology

I Bineva¹, D Nesheva¹, B Pejova², M Mineva¹, Z Levi¹ and Z Aneva¹

¹Institute of Solid State Physics, Bulgarian Academy of Sciences, 72 Tzarigradsko chaussee blvd, 1784 Sofia, Bulgaria

²Institute of Chemistry, Faculty of Science, Sts. Cyril and Methodius University, Skopje, Macedonia

E-mail: irka@issp.bas.bg

Abstract. Single layers of $Zn_xCd_{1-x}Se$ with various compositions ($x = 0.39, 0.59$ and 0.8) were prepared by thermal vacuum evaporation at room substrate temperature. Consecutive deposition of small portions of ZnSe and CdSe with equivalent thickness of 0.12 or 0.37 nm was applied. X-ray diffraction and atomic force microscopy measurements were applied to explore the evolution of the crystal structure, microstructure, composition and surface morphology upon furnace annealing at 200 °C and 400 °C in an inert atmosphere. It has been found that as-deposited films were nanocrystalline with a grain size of around 10 nm and cubic structure. Upon annealing the size increased approximately three times and the cubic structure was preserved; no appearance of wurtzite phase was observed. It has been also ascertained that annealing caused significant reduction of the film surface roughness. Atomic force microscopy phase images revealed existence of a second phase on the surface of as-deposited films which disappeared after annealing. The effect of the preparation conditions on the film properties and annealing induced changes is discussed.

1. Introduction

The detection of blue-UV light has traditionally been the province of photomultiplier tubes, which are sensitive and fast but not well-suited for space and field applications as they are fragile and require high voltages. Enhanced Si detectors are thus often used, but their relatively low band gap results in high reflectivity, and dark currents that require cooling to improve sensitivity. This has led to interest in the prospects for II-VI [1,2] or III-V materials in short-wavelength detectors. The $Zn_xCd_{1-x}Se$ II-VI ternary alloys are direct-gap semiconductors in which the optical bandgap variation spans the entire visible range (from 1.75 to 2.7 eV) and the lattice parameter gradually decreases as the Zn content, x , is varied between 0 and 1. The bandgap tunability of the $Zn_xCd_{1-x}Se(S)$ systems means that they are candidates for use in tandem solar cells [3,4]. A more recent potential application of semiconductor thin films is in the generation of Terahertz radiation from photoconductive antennae.

For the preparation of ternary II-VI semiconductor layers mainly molecular beam epitaxy [5,6] and electrodeposition [7,8] techniques are used. On the other hand thermal evaporation in vacuum allows deposition of films with a low contamination level at a relative low cost. In previous papers [9,10] we have reported an original approach for preparation of $Zn_xCd_{1-x}Se$ thin films of various compositions in the range $x = 0.39 - 0.8$. The films were produced by alloying of ultra thin ZnSe and

CdSe films and the compositional variation were achieved by varying the equivalent thickness of the films.

In this study $Zn_xCd_{1-x}Se$ thin films with three different compositions are prepared by thermal vacuum evaporation and the effect of furnace annealing at 200 °C and 400 °C on the crystal structure, microstructure and surface morphology of the films is explored.

2. Experimental details

Simultaneous thermal evaporation of ZnSe and CdSe powders (Merk, Suprapure) from two independent tantalum crucibles was applied for the preparation of $Zn_xCd_{1-x}Se$ layers with $x = 0.39, 0.59$ and 0.8 and thickness of 400 nm. The layers were deposited on Corning 7059 glass substrates kept at room temperature. During the film deposition the substrates were rotated at a rate of 20 turns/min. During each turn pass they spent over each crucible 1/12 of the turn time and the time between the consecutive deposition of CdSe and ZnSe is 5/12 of the turn time. The film composition was set by using appropriate deposition rate (0.5 or 1.5 nm/sec) for each material. The rates were controlled by two previously calibrated quartz microbalance systems MIKI FFV. Thus, consecutively deposited small portions of ZnSe/CdSe with equivalent thickness of around 0.12/0.37, 0.37/0.37 and 0.37/0.12 nm made $Zn_xCd_{1-x}Se$ alloys with $x = 0.39, 0.59$ and 0.8 , respectively. More details on the deposition procedure can be found in [9,10]. For each composition a part of the films were furnace annealed for 60 min in an argon atmosphere at annealing temperature $T_a = 200$ °C or 400 °C.

XRD experiments were performed on a Rigaku Ultima IV diffractometer with Cu K_α radiation, $\lambda = 0.154$ nm. The XRD patterns were registered via the step method applying 0.02° steps (2θ) and a counting time of 0.6 sec/step. The scattered X-ray radiation was detected with DteX detector. All the XRD patterns were taken within an angular interval 2θ from 10° to 80° where the main diffraction peaks of ZnSe and CdSe are located.

A Veeco Multimode V scanning probe microscope operating in tapping mode was used to investigate the surface morphology and phase composition of the $Zn_xCd_{1-x}Se$ films. Height, amplitude error and phase images were recorded in 500 nm, 1 μm and 5 μm scale. The scan rate was in the range 1 - 2 Hz and the image resolution was 512 lines per scan direction for the 1 μm and 5 μm images and 1024 lines for the 500 nm ones. At least three different points on the sample surface were explored. Aluminum coated silicon cantilevers TAP150-Al-G for soft tapping mode with a nominal resonance frequency of 150 kHz and a typical force constant of 5 N/m were used; the tip radius is less than 10 nm. All images were just flattened and no further processing was carried out. Roughness measurements were performed using the Nanoscope 7.30 programme. The grain size analysis was done on 500 nm images with SPIPtm image processing software version 6.0.4 (Image metrology A/S) – evaluation copy, using Watershed method.

3. Results and Discussion

3.1. X-ray diffraction

In figure 1 (a) XRD patterns of as-deposited $Zn_xCd_{1-x}Se$ layers with $x = 0.39, 0.59$ and 0.8 are shown. The shape of all the patterns is typical for materials with polycrystalline structure. The diffraction peak at 2θ in the range $26-27^\circ$ is the most intensive, narrow and well pronounced. Two additional very weak peaks at about 44° and 52° are also seen. The three peaks correspond to the $\{111\}$, $\{220\}$ and $\{311\}$ families of crystallographic planes in cubic $Zn_xCd_{1-x}Se$ [10]. The absence in the experimental patterns of peaks, which should correspond to $\{100\}$, $\{101\}$ and $\{102\}$ families (at around 24° , 29° and 37° , respectively) in the crystallographic planes of wurtzite $Zn_xCd_{1-x}Se$, clearly indicates that the films with all compositions have cubic symmetry. Based on the big difference in the peaks' intensity in figure 1 one can suggest that the films have a preferential $\{111\}$ orientation.

The peak $\{111\}$ is presented in an enlarged scale in figure 1 (b), which reveals that the decrease in the Zn content causes a proportional shift of the peak to lower angles. This shift is due to the substitution of Zn with Cd atoms that leads to an increase in the lattice parameter a (the cubic

modifications of ZnSe and CdSe are isomorphous and completely soluble in the solid state). In order to get quantitative information about the {111} diffraction peaks all XRD spectra were background corrected and then least-square fitted for the estimation of their angular position, full width at half maximum (FWHM), area and height. Two analytical functions, Gaussian and Lorentzian, were initially tried for fitting, with better results obtained by applying the Lorentzian one. The results obtained from the Lorentzian fitting of the spectra of as-deposited films are summarised in table 1 and the peak positions are shown in figure 1 (b), inset. The dashed line in the inset represents the standard relationship between the {111} peak position and the Zn content x obtained using Bragg's equation $d_{\{hkl\}} = \lambda/2\sin\theta$ and taking into account that the lattice constant in cubic crystals $a = d_{\{hkl\}}(h^2+k^2+l^2)^{1/2}$ (h, k, l are the lattice planes; $d_{\{hkl\}}$ is the corresponding interplanar distance; for the {111} peak $a = d_{\{111\}}\sqrt{3}$) obeys Vegard's rule $a = x a_{\text{ZnSe}} + (1-x) a_{\text{CdSe}}$ [11]. It is seen from the inset that the experimental points are fairly close to this line, which confirms that the suggested technique allows fabrication of $\text{Zn}_x\text{Cd}_{1-x}\text{Se}$ films with a good composition control.

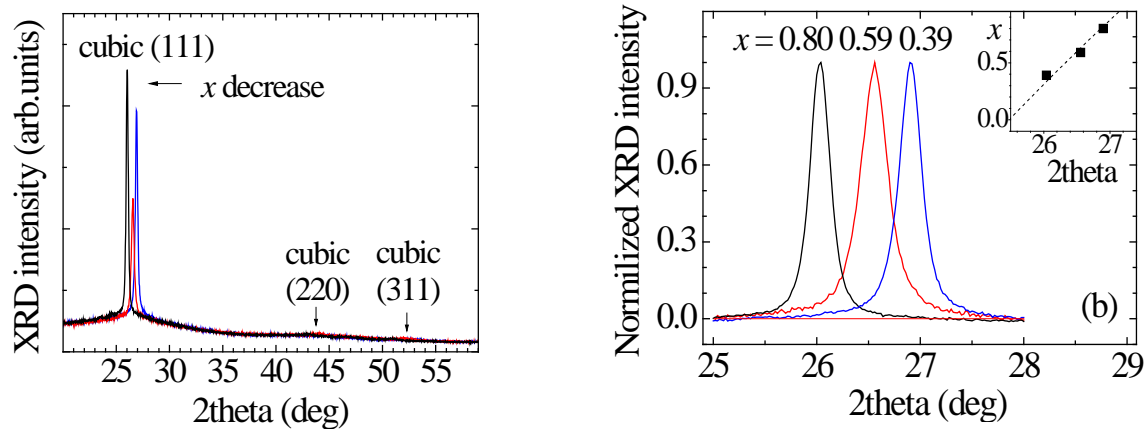


Figure 1. (a) XRD spectra of three as-deposited $\text{Zn}_x\text{Cd}_{1-x}\text{Se}$ films with different compositions; (b) a part of the pattern showing the {111} peak. Inset: the dashed line represents the relationship between the {111} peak position and the Zn content x , the symbols correspond to the experimental positions.

Table 1. Angular position, lattice constant, full width at half maximum, area and height of as-deposited and annealed $\text{Zn}_x\text{Cd}_{1-x}\text{Se}$ thin films determined by Lorentzian fit of the {111} peak in the XRD spectra.

$\text{Zn}_x\text{Cd}_{1-x}\text{Se}$	Annealing	Center (deg)	Lattice constant (nm)	FWHM (deg)	Area	Height
$x = 0.8$	as-deposited	26.91	0.5734	0.245	13253	34391
	$T_a = 200\text{ }^\circ\text{C}$	27.02	-	0.254	14235	35700
	$T_a = 400\text{ }^\circ\text{C}$	27.01	0.5713	0.259	14371	35300
$x = 0.59$	as-deposited	26.55	0.5808	0.324	10008	19650
	$T_a = 200\text{ }^\circ\text{C}$	26.56	-	0.296	10261	22043
	$T_a = 400\text{ }^\circ\text{C}$	26.63	0.5791	0.269	11465	27068
$x = 0.39$	as-deposited	26.03	0.5922	0.211	13956	42017
	$T_a = 200\text{ }^\circ\text{C}$	26.10	0.5906	0.201	14366	45515
	$T_a = 400\text{ }^\circ\text{C}$	26.07	-	0.196	19555	63630

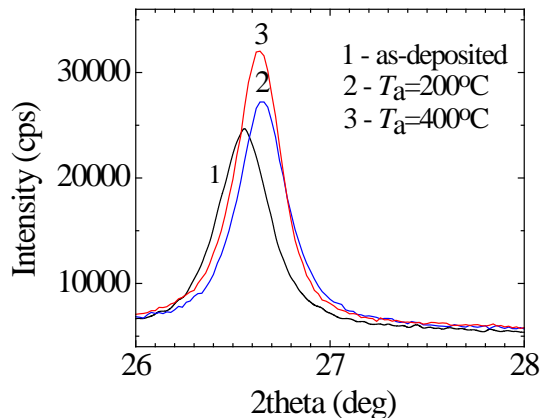


Figure 2. XRD spectra of three $Zn_xCd_{1-x}Se$ films with $x = 0.59$: 1 - as-deposited, 2 - annealed at 200 °C, 3 - annealed at 400 °C.

Figure 2 depicts the {111} peaks of an as-deposited $Zn_xCd_{1-x}Se$ film with $x = 0.59$ and two annealed films. It is seen that upon annealing the {111} peak slightly shifts to the larger angles and its intensity increases. Similar changes have been observed for the other two compositions. The results from the Lorentzian fitting (table 1) show that upon annealing the {111} peak displays a shift of 0.07° to 0.1° (in 2θ scale), which corresponds to a lattice constant decrease of 0.016-0.021 nm and in addition the annealing causes an increase of the peak area. These observations indicate an improvement of the film crystallinity, which is expected [12], as well as a slight densification. Since CdSe and ZnSe single crystals are usually characterized by the hexagonal wurtzite structure, normally the annealing induces a transition from cubic to hexagonal structure and also an increase of the grain size [12]. However, in our case even the films annealed at 400 °C show a cubic structure. In a previous study on the structure of self assembled CdSe nanocrystals embedded in a SiO_x matrix we revealed [13] that three quarters of nanocrystals in as-deposited films (grown at room substrate temperature) are of hexagonal structure and one quarter were cubic or both lattice types. For the samples annealed at 400 °C it was determined one half of the particles with cubic structure and another half with hexagonal or both lattice types [13]. These quite unusual observations give us basis to adopt the assumption made in [12] that the nanoparticle surface properties affect significantly their structure. Perhaps, the preparation technique we applied determines certain nanoparticle surface properties which impede cubic to hexagonal transformation. Annealing at higher T_a and/or longer annealing times will be carried out to verify this assumption. As for the grain size, it is frequently estimated from the FWHM of XRD bands. As seen from table 1 the annealing of the films with $x = 0.39$ and 0.8 causes a gradual FWHM decrease but an increase is observed for the films with $x = 0.59$. The obtained FWHM alterations are quite small and they are normally affected by both the grain size and fixed residual stress in the films. Therefore the annealing induced changes in the film microstructure, surface roughness and phase composition were explored by AFM measurements.

3.2. Atomic force microscopy

Two-dimensional surface images of two films with $x = 0.39$, as-deposited and annealed at 400 °C, are depicted in figure 3. They reveal that the layers are nanocrystalline and show an increase of the grain size upon annealing. Size increase has been observed for the films with all compositions. The obtained grain size of as-deposited films is around 10 nm while in the annealed samples the size is three times greater (~ 30 nm). The small grain size in the as-deposited films implies a high density of embryonic grains on the substrate surface which may be due to the applied deposition technique. Perhaps, the embryo density is high because of the combination of the very low average deposition rate and the low substrate temperature, resulting in low mobility of ad-atoms on the substrate surface.

Another effect observed upon the film annealing is a decrease of the surface roughness. It is illustrated in figure 4 for the films with $x = 0.8$. In as-deposited films a growth of quite high spikes is observed whose density is highest in the films with $x = 0.8$ (figure 4 (a)). Perhaps the low substrate

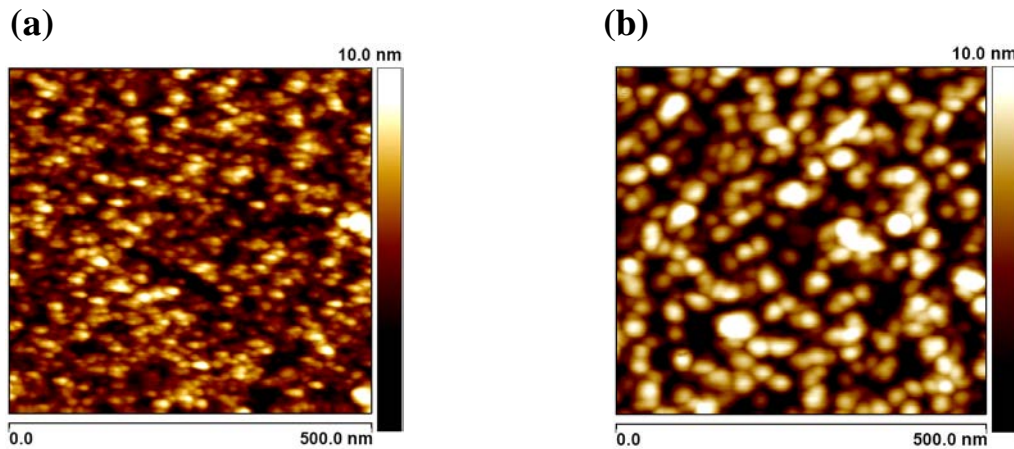


Figure 3. Two-dimensional surface images of two $\text{Zn}_x\text{Cd}_{1-x}\text{Se}$ thin films with $x = 0.39$: (a) as-deposited and (b) annealed at $400\text{ }^\circ\text{C}$. The scale of both pictures is 500 nm in lateral direction and 10 nm in height.

temperatures, i.e. the low ad-atoms mobility, facilitate the spikes growth. The annealing at $200\text{ }^\circ\text{C}$ significantly improves the surface smoothness (figure 4 (b)); a decrease of the root mean square roughness from 4.5 , 6.9 and 6.0 nm to 1.3 , 2.1 and 1.6 nm for films with $x = 0.8$, 0.59 and 0.39 , respectively, has been observed on $5 \times 5\ \mu\text{m}^2$ surface area. The annealing at $400\text{ }^\circ\text{C}$ results in some roughness increase (figure 4 (c)), which may be due to some re-evaporation of Se from the film surface.

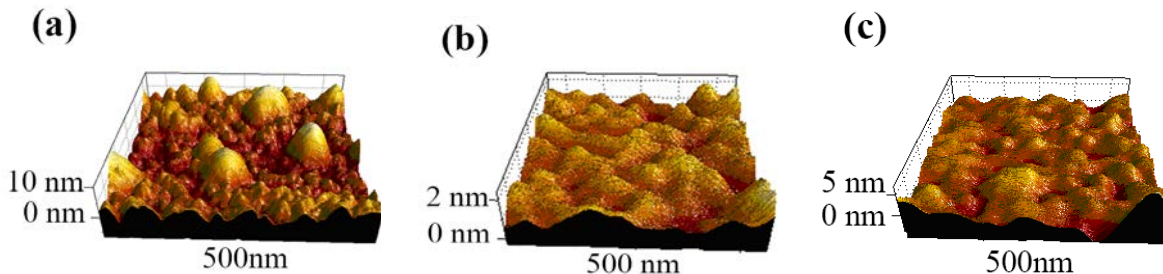


Figure 4. Three-dimensional surface images of three $\text{Zn}_x\text{Cd}_{1-x}\text{Se}$ films with $x = 0.8$: (a) as-deposited, (b) annealed at $200\text{ }^\circ\text{C}$, (c) annealed at $400\text{ }^\circ\text{C}$.

Finally, we would like to consider the compositional homogeneity of the films as seen from the surface phase images. Figure 5 depicts the phase images of as-deposited and annealed $\text{Zn}_x\text{Cd}_{1-x}\text{Se}$ films with $x = 0.59$. The phase signal is sensitive to variations in composition, adhesion, friction, viscoelasticity as well as other factors. Two different phases have been observed in all as-deposited films. The amount of the second phase (white colour) is highest in the films with $x = 0.59$ while in the films with the other two compositions it is relative small. This observation can be understood keeping in mind that the films with $x = 0.59$ were formed by allowing of ZnSe/CdSe layers with an equivalent thickness of 0.37 nm while in the films with $x = 0.39$ and 0.8 the equivalent thickness of one material is 0.12 nm . The registration of nanosized second phase on the film surface is in agreement with the conclusion made for the volume from Raman scattering experiments for existence of nanosized Cd-enriched regions [10]. Based on figure 5 (b) one can think that the applied annealing at $200\text{ }^\circ\text{C}$ is not enough for full composition homogenization in the films with $x = 0.59$; it occurs at $T_a = 400\text{ }^\circ\text{C}$. For the other compositions the second phase has not been seen upon annealing at $T_a = 200\text{ }^\circ\text{C}$.

The observed small grain size makes as-deposited films interesting for chemical sensor applications because the integral interface area in such films is very large. Previous investigations on CdSe films annealed at 400 °C have revealed [14] dark conductivity increase and decrease in the

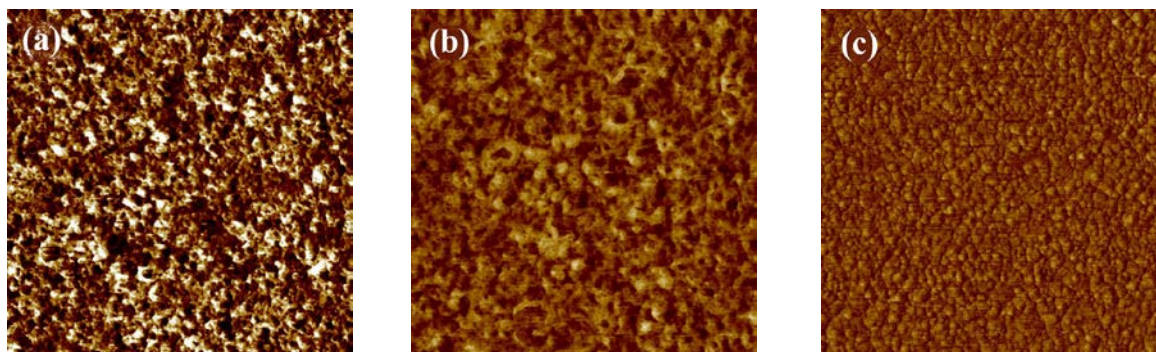


Figure 5. Phase surface images of three $Zn_xCd_{1-x}Se$ films with $x = 0.59$: (a) as-deposited, (b) annealed at 200 °C and (c) annealed at 400 °C. The scale of all pictures is 1 μm in lateral direction.

density of ‘slow’ recombination centres. It may be expected that the above described annealing induced size increase in $Zn_xCd_{1-x}Se$ films will cause similar dark and photoconductivity changes and its combination with the observed effects of composition homogenization and surface smoothening increases the potential of the $Zn_xCd_{1-x}Se$ layers for application in short-wavelength detectors and solar cells.

4. Conclusions

Single layers of $Zn_xCd_{1-x}Se$ with $x = 0.39, 0.59$ and 0.8 were prepared by thermal evaporation of ZnSe and CdSe in vacuum. X-ray diffraction and AFM measurements revealed that as-deposited films are nanocrystalline with cubic structure and a small grain size (~ 10 nm). These observations have been related to the low substrate temperature and low average deposition rate. The annealing at 400 °C for 60 min resulted in size increase (approximately three times) but wurtzite phase was not detected. It has been assumed that the specific preparation approach determines certain nanoparticle surface properties which impede cubic to hexagonal transformation. Atomic force microscopy height images have shown spikes on the surface of as-deposited films whose density depends on the composition. The spikes growth has been assigned to low ad-atoms mobility during the film deposition. An anticipated roughness reduction has been observed upon annealing at 200 °C while the annealing at 400 °C caused some roughness increase related to re-evaporation of Se atoms. AFM phase images have revealed existence of a second phase on the surface of as-deposited films which disappeared after annealing. The largest amount of the second phase has been observed in the films with $x = 0.59$. This result has been related to the relative large equivalent thickness (0.37 nm) of both ZnSe and CdSe sublayers.

Acknowledgements This work has been financially supported by the Bulgarian Ministry of Education, Youth and Science under grant DMU 03-91.

References

- [1] Hsiao C H, Changn S J, Hung S C, Cheng Y C, Huang B R, Wang S B and Lan B W 2010 *J. Cryst. Growth* **312** 1670
- [2] Yoon Y-J, Park K-S, Heo J-H, Park J-G, Nahm S and Choi K J 2010 *J. Mater. Chem.* **20** 2386
- [3] Tamargo M C (ed) 2002 *II–VI Semiconductor Materials and their Applications* (New York: Taylor and Francis) ch 2
- [4] Chandramohan R, Mahalingam T, Chu J P and Sebastian P J 2004 *Sol. Energy Mater. Sol. Cells* **81** 371

- [5] Gupta P, Maiti B, Maity A B, Chaudhuri S and Pal A K 1995 *Thin Solid Films* **260** 75
- [6] Hankare P P, Chate P A, Asabe M R, Deleka S D, Mulla I S and Garadkar K M J 2006 *J. Mater. Sci.: Mater. Electron.* **17** 1055
- [7] Katayama K *et al* 2000 *J. Cryst. Growth* **214–215** 1064
- [8] Chen W R and Huang Ch J 2004 *IEEE Photon. Technol. Lett.* **16** 1259
- [9] Nesheva D, Aneva Z, Šćepanović M J, Bineva I, Levi Z, Popović Z V and Pejova B 2012 *J. Phys.: Conf. Series* **253** 012035
- [10] Nesheva D, Aneva Z, Šćepanović M J, Levi Z, Iordanova I and Popović Z V 2011 *J. Phys. D* **44** 415305
- [11] Bis R F and Dixon J R 1969 *J. Appl. Phys.* **40** 1918
- [12] R. J. Bandaranayake, G. W. Wen, J. Y. Lin, H. X. Jiang and C. M. Sorensen 1995 *Appl. Phys. Lett.* **67** 7
- [13] Hofmeister H, Nesheva D, Levi Z, Hopfe S and Matthias S 2000 *Proc. EUREM 12*, Brno, Eds. Frank C L and Ciampor F (Brno: Czechoslovak Society for Electron Microscopy) p.365
- [14] Nesheva D, Reynolds S, Aneva Z, Main C and Levi Z 2005 *J. Optoelect. Adv. Mat.* **7** 517